Likelihood Surface Preprocessing with the JPDA Algorithm: Metron Data Set

David W. Krout
Applied Physics Lab
University of Washington
Seattle, WA, U.S.A.
dkrout@apl.washington.edu

Evan Hanusa
Electrical Engineering
University of Washington
Seattle, WA, U.S.A.
hanusaem@ee.washington.edu

Abstract – *This paper presents tracking results on the Metron data set using the JPDA algorithm and a preprocessing likelihood surface formulation. The Metron data set is a simulated data set and is designed to be very difficult with large bearing and range errors which leads to high localization error for true detections. There are also significant amounts of clutter. Results using other data association algorithms such as the PDA, PDAFAI, and PDAFAIwTS were not good, which led to the use of a likelihood surface. The preprocessing step using the likelihood surface is key for achieving reasonable results. For the baseline tracking scenario where the truth is known, the results were encouraging. Extending this technique to include acoustic modeling and Doppler information will be topics of future research.*

Keywords: Tracking, filtering, estimation.

1 Introduction

This paper presents results of a Joint Probailistic Data Assocation (JPDA) tracker on the Metron data set. A likelihood surface pre-processing step is used in the algorithm and is key to getting reasonable results. In previous work a sonar tracking algorithm was adapted to the acoustic propagation environment [1, 2]. Results for the PDAFAIwTS on the TNO Blind data set and the SEABAR '07 sea trial were presented in [3]. The TNO blind data set was created by researchers at TNO Defence, Security and Safety (The Hague, The Netherlands) for use by the Multi-Static Tracking Working Group (MSTWG). The SEABAR '07 sea trial was an experiment conducted by the NATO Undersea Research Lab (NURC) [4, 5] on the Malta Plateau. The latest data set was created by Metron to be used by members of the MSTWG and will be the focus of this paper.

Initial testing of the Metron data set using the Probabilistic Data Association (PDA), Probabilistic Data Association Filter with Amplitude Information (PDAFAI) [6, 7], and PDAFAI with Target Strength (PDAFAIwTS) algorithms showed less than desirable results. The Metron data set is a very difficult data set with large timing errors and bearing errors. The large errors combined with a considerable amount of false contacts makes for a very difficult data set. Further details will be presented in section 2.

Section 2 will summarize the Metron data set. Section 3 of this paper will review the mathematical basis for the Joint Probabilistic Data Association algorithm. Section 4 will summarize the likelihood surface formulation used in the pre-processing. Section 5 will show the tracking results from the Metron data set. Section 6 will summarize the paper and discuss areas of continued work.

2 Metron Data Set

The Metron data set [8] was created by Metron (http://www.metsci.com/) for the MSTWG. It is a simulated data set with five distinct scenarios. The truth was known for scenario 1 and scenario 4, and the remaining four scenarios were 'blind', meaning the true target locations (and the number of targets, 8 max) were unknown. The ground truth plot for scenario 1 is shown in Figure 1, which is from the source document for the data set [8]. There were four targets in this scenario as shown in the figure. The ground truth plot for scenario 4 will be shown in the results section.

The sensor layout for the simulations is based on a distributed number of underwater sensors where there are sources and receivers. The blue circles are the receivers and the blue asterisks are the sources. There are 4 sources and 25 receivers. The sensor layout is the same for all the scenarios. The ping rate is 180 seconds for a duration of 200 pings (10 hours). The ping schedule follows a preset list which cycles through all the sources sequentially and repeatedly. There are FM and CW transmissions simulated (alternating each ping for each source), and in this paper all contacts are used in the tracking algorithms. Although it is not clear from the figure, the targets travel four times around each of their designated square paths.

The contact measurements were generated using the following parameters:

- Sound speed of 1500 m/s
- Bearing error is normally distributed with mean 0.0 and standard deviation 8.0

- Time difference of arrival (TDOA) error is normally distributed with mean 0.0 s and standard deviation 0.4 s
- Bistatic Doppler error is normally distributed with mean 0.0 m/s and standard deviation 0.5 m/s (CW only)
- Maximum of 8 targets
- Constant sound speed
- 200 ping periods, 180 seconds per period
- Blanking zone of 1 second

The bearing error and TDOA error become quite clear when looking at the contacts for one ping as shown in Figure 2. The pink dotted lines show which receiver the contact was originated from. Due to the bearing and TDOA errors, the localization error of a contact can be quite large. For example, in Fig. 2 one of the contacts is almost 20km from the true target location. This kind of bearing error presents a difficult tracking scenario and mixing in false contacts makes matters even worse.

Another issue that makes the data set difficult is the low overall probability of detection, especially when viewed from a centralized tracking standpoint. There are a large number of source/receiver pairs with detection opportunities, but limited number of true detections. Selecting the M/N/K parameters for track management, is a difficult problem because of the multistatic field. With previous data sets, a rule of thumb would be 3 detections out of 5 opportunities. However for this data set the number of opportunities had to be greatly increased to take into account the large number of receivers and the round robin ping cycle.

3 Joint Probabilistic Data Association Filter

JPDA [9] is an extension of PDA to allow for multiple targets. After initial testing of the PDA, PDAFAI, and PDAFAIwTS algorithms with the Metron data set did not produce good results, the algorithms were extended to the JPDA algorithm. The amplitude and Target Strenth (TS) portions of the algorithms were not initially tested, but will be an area of future work. The desire was that by extending to the JPDA, results would be improved. However, the difficulties of the Metron data set were not overcome by the JPDA alone.

This description of the JPDA algorithm assumes an underlying Kalman Filter. This can be modified to include the extended Kalman Filter (EKF) or the unscented Kalman Filter(UKF), but an unmodified Kalman filter is shown below for ease of explanation.

The state at time k is predicted:

$$\begin{aligned} x_i(k|k-1) &= Fx(k-1), \\ P(k|k-1) &= FP(k-1)F^T + Q, \end{aligned} \quad (1)$$

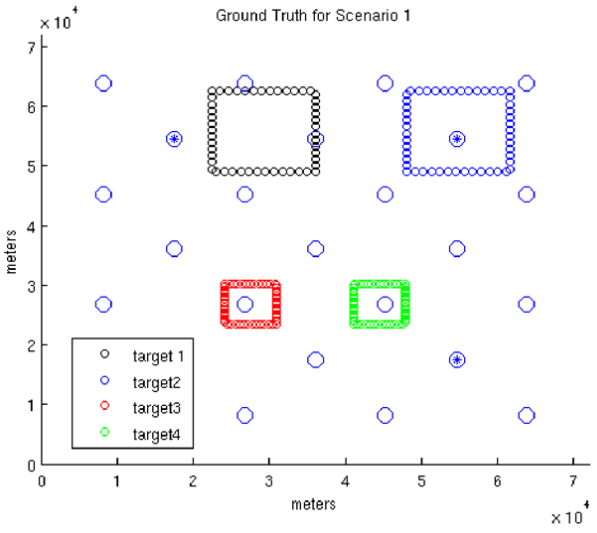

Figure 1: Ground truth plot and sensor layout for scenario 1 of the Metron data set. Four targets are present that travel in four loops following the rectangular paths. There are 4 sources (blue asterisks) and 25 receivers (blue circles).

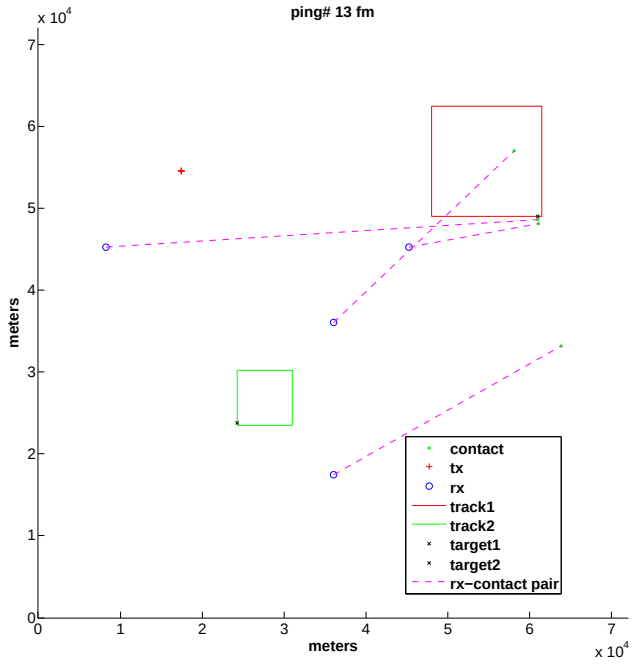

Figure 2: The target detections from the FM ping (Ping #13) are shown in this plot. The magenta dotted lines show which receiver the contact originated from. One of the contacts is almost 20km away from the true target location.

where F is the motion model, P is the covariance matrix, and Q is the process noise.

The residuals, $\tilde{y}_{ij}$, are calculated between gated contacts y_j and the predicted target location:

$$\tilde{y}_{ij} = y_j(k) - Hx_i(k|k-1),$$

where H is the measurement matrix.

The distance, d_{ij}, is calculated for all gated contacts, j, using the residual covariance S_i from the Kalman Filter. The distances are scored using the Gaussian pdf assumtpion:

$$\begin{aligned} d_{ij}^2 &= \tilde{y}_{ij}^T \mathbf{S}_i^{-1} \tilde{y}_{ij}, \\ g_{ij} &= \frac{e^{-d_{ij}^2/2}}{(2\pi)^{M/2}\sqrt{|S_i|}}, \end{aligned} \quad (2)$$

where g_{ij} is the distance score, and M is the spatial dimension (2 in this example).

The probability of the data, Y^k, given an association, A, is calculated by:

$$P(Y^k|A) = \frac{C^{N_{fa}}}{c} \prod_{j:g_{ij}>0} (g_{ij}) P_D^{N_d} (1-P_D)^{N_m}, \quad (3)$$

where C is the density of false contacts, N_{fa} is the number of false contacts, c is the normalizing constant, P_D is the probability of detection, N_d is the number of tracks that have a contact associated, and N_m is the number of tracks without an associated contact.

The association weight, β_{ij} is the sum of the probabilities of all the association , M_{ij}, that associate contact j with track i:

$$\begin{aligned} \beta_{ij} &= \sum_A P(Y^k|A) M_{ij}(A), j > 0, \\ \beta_{i0} &= 1 - \sum_{j>0} \beta_{ij}. \end{aligned} \quad (4)$$

These values for β_{ij} are used in the same way as standard PDA:

$$\tilde{y}_i = \sum_j \beta_{ij} \tilde{y}_{ij}. \quad (5)$$

3.1 Additional Tracking Details

- Track management is handled using an M/N/K style logic. M is the number of consecutive pings for a track to be confirmed. N is the number of missed consecutive detections to delete an unconfirmed track. K is the number of missed detections for a confirmed track to be deleted. The parameters that were used were chosen primary by trial and error and will be reported with the tracking results.

- Tracking architecture is centralized.

- The gate size and the probability of detection parameters also play a role in the performance of the tracking algorithm. The values for each simulation run will be specified with the results.

- The number of maxima chosen after the likelihood surface preprocessing is also an input parameter that can be set. The likelihood surface process will be discussed in the next section, and the number of maxima was chosen to be 30 for all the results in this paper. Including more than 30 maxima did not appear to improve the tracking results.

4 Likelihood Surface

The initial testing of the Metron data set using the PDA, PDAFAI [6, 7], and the PDAFAIwTS algorithms did not produce very good results. There were many false tracks, so many that even if the true targets were tracked, they were indistinguishable. In order to mitigate the overwhelming amount of false tracks created, a pre-processing step utilizing a likelihood surface was used. The likelihood surface formulation will be described next.

The likelihood surfaces are calculated for each of the j contact locations, b_{ij}, r_{ij}, where b is the bearing and r is the range. The error statistics for each receiver, i, are used in the formulation. I_i is an indicator variable which indicates whether or not the true contact was actually detected.

$$\begin{aligned} &L\left(c_{(x,y)}|b_{ij}, r_{ij}, I_i = 1\right) = \\ &(2\pi\sigma_b\sigma_r)^{-1} exp\left(\frac{-\left(b_{(x,y)}-b_{ij}\right)^2\left(r_{(x,y)}-r_{ij}\right)^2}{2\sigma_b^2\sigma_r^2}\right), \end{aligned} \quad (6)$$

where $c_{(x,y)}$ is any location in the likelihood surface, $b_{(x,y)}$ is the bearing at (x, y) for i^{th} receiver, $r_{(x,y)}$ is the bistatic range at (x, y) for the i^{th} receiver, σ_b is the bearing covariance, and σ_r is the range covariance.

Each receiver's total likelihood surface given that the true contact was detected is calculated by summing over all j contacts for each receiver.

$$L\left(c_{(x,y)}|\bar{b}_i, \bar{r}_i, I_i = 1\right) = \sum_{j=1}^{n} L\left(c_{(x,y)}|b_{ij}, r_{ij}\right) \quad (7)$$

Each receiver's probability of detection surface $p_{Di}(x, y)$ is the probability that a contact at (x,y) will be detected. The total likelihood of a contact being at (x, y) is calculated in equation 8, where $L(c_{(x,y)}|I_i = 0)$ is the probability that a contact is at (x, y) and not detected. We chose $L(c_{(x,y)}|I_i = 0)$ as a small constant, 1e-8. This value could be tweaked to be location dependent in a scenario where additional information is known (bathymetry, for example).

$$\begin{aligned} &L\left(c_{(x,y)}|\bar{b}_i, \bar{r}_i\right) = \\ &L\left(c_{(x,y)}|\bar{b}_i, \bar{r}_i, I_i = 1\right) p_{Di}(x, y) + \\ &L(c_{(x,y)}|I_i = 0)\left(1 - p_{Di}(x, y)\right) \end{aligned} \quad (8)$$

The combined likelihood surface is calculated as in equation 9.

$$L\left(c_{(x,y)}|\bar{b}_{1..m}, \bar{r}_{1..m}\right) = \prod_{i=1}^{m} L\left(c_{(x,y)}|\bar{b}_i, \bar{r}_i\right) \quad (9)$$

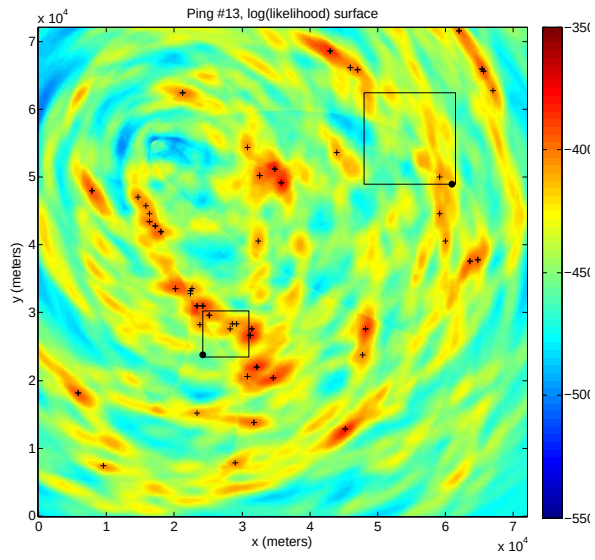

Figure 3: The log of the likelihood surface for ping #13. The large black boxes are the true target paths. The true locations for two of the targets are plotted with the black dots. The black plus signs are the 30 maxima of the likelihood surface

The top 30 local maxima of the likelihood surface are then calculated and sent to the JPDA tracking algorithm. These maxima are found by running a 3x3 window over the likelihood surface - if the center of the 3x3 window is the maximum value in that window, it is considered a local maximum. It is noted that there are other techniques for approximating the maxima of a likelihood surface. The authors are currently exploring some of these techniques [10], including a Gaussian mixture approximation. As stated earlier, choosing to use 30 maxima is arbitrary, however when more maxima were chosen the tracking results were not significantly different. When less than 30 were chosen the results were negatively affected some of the time. An example of the likelihood surface is shown in Figure 3. The log of the likelihood is plotted for ease of viewing. The black lines are the true target paths and the black dots are the true target locations (two of the targets) at the time of the 13th ping. The 30 maxima are marked with black plus signs. There are several peaks near the target path in the lower left-hand corner, however there were none at the true target position. There is a peak near the true target location in the upper right which is a result of true detections.

4.1 Blanking Region

The simulation included a blanking zone of one second. This results in an ellipse around the transmitter and receiver in which no contacts can be detected. When the likelihood surface is formed using the contact locations, this blanking region will have zero likelihood. If this is not accounted for, then large areas of each receiver's likelihood surface will be zero, and the resulting combination will be zero nearly everywhere inside the simulation area. This is accounted for in equation 8 with the term $L(c_{(x,y)}|I_i = 0)$. This is the probability that a contact is at location (x, y), but not detected.

5 Tracking Results

Results will now be presented on the Metron data set. Results will be presented for all five scenarios for completeness even though the truth is unknown for all the scenarios. The truth for scenario one was known *a priori* and was used to provide feedback on how well the tracking algorithms were performing on a baseline scenario. The truth for scenario four was provided after initial results were presented, and was not used to tune any tracking parameters in the reporting of the results in the paper. The truth for the remaining scenarios will be provided at a later date and will be reported on in future publications. The truth data for scenario 4 is shown in figure 8.

The MSTWG metrics calculated for scenario 1 and 4 are based on the metrics in [11] developed for the MSTWG. The likelihood surface preprocessing step provides a different set of contacts than the originals which do not include the associated truth flags. An algorithm had to be determined which would fairly determine which maxima were from true contacts, then the metrics could be calculated. To determine which maxima would be considered true contacts for the metric calculation, the following method was used. At each time step, for each target i, the mean contact location, μ_i was calculated over all receivers that received a contact from that target.

$$\mu_i = \gamma^{-1} \sum_j c_{ij}, \tag{10}$$

where c is a contact for a target i and reciever j, γ is the number of receivers that received a contact from target i in that ping. For each target i, the closest maximum to μ_i was chosen as the true contact for that ping. If the closest maximum was at a distance greater than a maximum distance of $1e4$ meters, then it was considered to be a missed detection.

The first test on the data set was using the true detections only. Figure 4 shows the tracking results for scenario 1 using the labeled data only. The true contacts were only labeled for the targets in the upper right and the lower left. The tracking algorithm is able to track the two targets, however there are significant errors in localization and many broken tracks.

As stated earlier, the JPDA algorithm without the preprocessing step does not perform well on this data set. This also includes other algorithms such as the PDA, PDAFAI, and the PDAFAIwTS [3]. These results will not be included in this paper. Figure 5 shows the tracking results for scenario 1 of the Metron data set using the JPDA algorithm with the pre-processing. The title of the figure contains the tracking parameters that were used. The 'numMaxima' is the number of maxima used, which was 30 for all the results in this paper. The M/N/K parameters are displayed as well as the gate size and probability of detection. The blue lines represent all the confirmed tracks for the entire duration of the

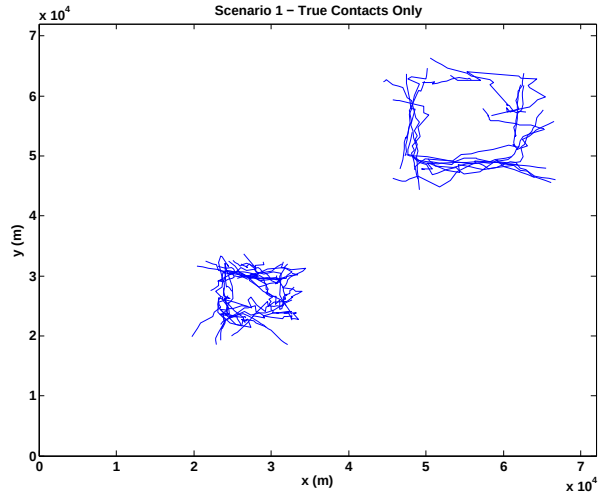

Figure 4: Tracking results for scenario 1 of the Metron data set, using only the true detections. The blue lines represent all the confirmed tracks for the entire duration of the simulation.

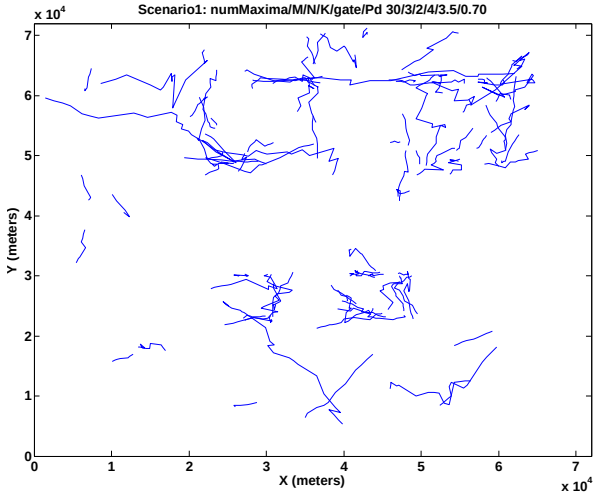

Figure 5: Tracking results for scenario 1 of the Metron data set. The blue lines represent all the confirmed tracks for the entire duration of the simulation.

simulation. The rectangular boxes are visible from the confirmed tracks. The complete tracking metrics for scenario 1 and 4 are reported in Tables 1 and 2.

Figures 6, 7, through 10 are the tracking results for scenarios 2, 3 and 5. It is difficult to make many conclusions about scenarios 2, 3 and 5 without the truth data, however they are included here for completeness. The plots shown in Figures 6, 7, through 10 were chosen based on several runs of the tracking algorithms with varied tracking parameters (M/N/K, Pd, Gate Size). There were trends in confirmed tracks when comparing the various runs which were used to select these particular results. Scenario 2 has a rectangular box pattern of confirmed tracks with some tracks within the box. This was seen in most of the simulations runs for scenario 2. There appears to be a fixed clutter point in scenario 5, similar to what is seen in scenario 4.

The tracking results for scenario 1 are shown in Figure 5. The tacking results for scenario 1 were not as good as hoped, but the targets are visible as seen in Figure 5. The truth for scenario 4 is shown in Figure 8 along with the tracking results in Figure 9. The scales for both of these figures are not the same. The tracking algorithm was able to track segments of the ships, however the target was more difficult. Segments of the target were tracked, but over all the results need improvement.

5.1 Metrics

The metrics and plots presented for scenarios 4 are from simulation runs before the truth data was known and the tracking parameters were not changed. The metrics were calculated based on the methods described above. Table 1 shows the per-target metric results for scenario 1. Track false alarm rate is 0.555, latency is $360s$, and execution ratio is 0.113. Table 2 shows the metric results for the single target in scenario 4. The target was tracked about a third of the time and the fragmentation was very low. There is clearly more work to be done with this data set.

Target	1	2	3	4
TPD	0.32	0.50	0.17	0.51
TLE	2.34e3	2.53e3	1.37e3	1.32e3
Frag	0.0088	0.0125	0.0037	0.0163

Table 1: Metric results for 4 targets in scenario 1. Track Probability of Detection (TPD), Track Localization Error (TLE), Track Fragmentation (Frag).

Target	1
TPD	0.355
TLE	3.18e3
Frag	0.0075
TFAR	0.15
Latency	720s

Table 2: Metric results for the single target in scenario 4. Track Probability of Detection (TPD), Track Localization Error (TLE), Track Fragmentation (Frag), Track False Alarm Rate (TFAR).

6 Conclusion

This paper presents techniques for overcoming the difficulties of the Metron data set. The results for Scenario 1 showed promising results although far from perfect. The results for scenario 4 also showed some signs of hope. The ships were tracked most of the time, however the target was

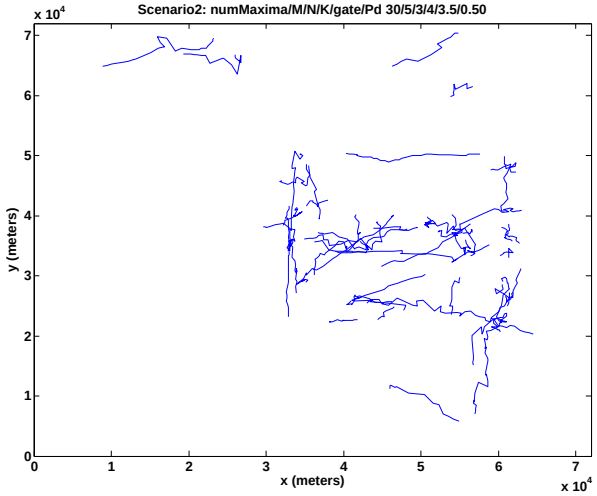

Figure 6: Tracking results for scenario 2 of the Metron data set. The blue lines represent all the confirmed tracks for the entire duration of the simulation.

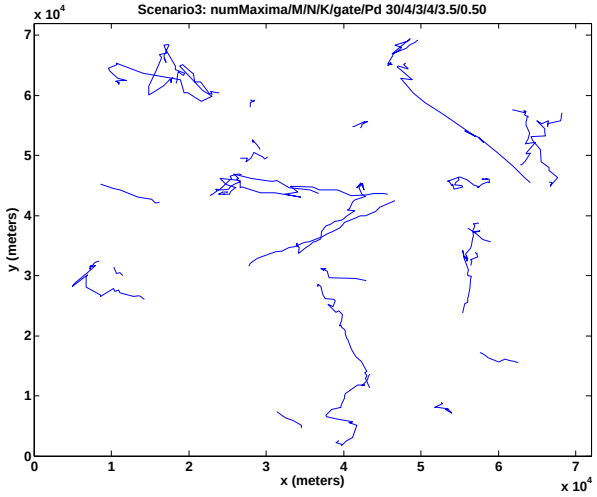

Figure 7: Tracking results for scenario 3 of the Metron data set. The blue lines represent all the confirmed tracks for the entire duration of the simulation.

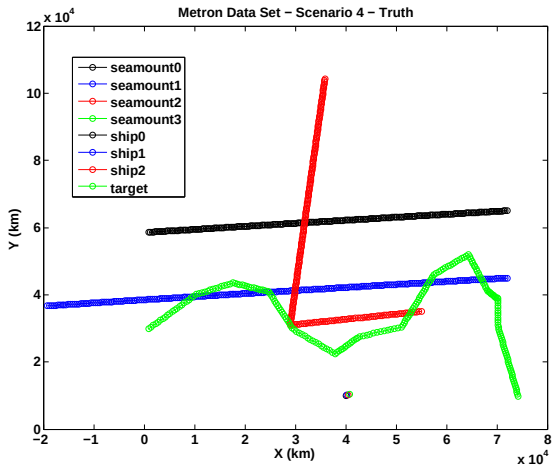

Figure 8: Ground truth plot for scenario 4 of the Metron data set.

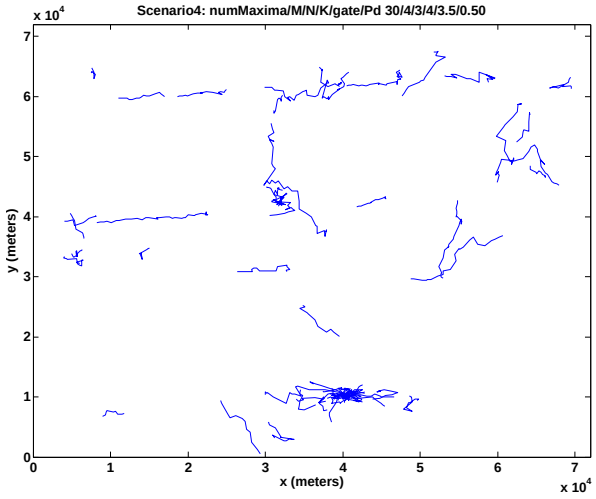

Figure 9: Tracking results for scenario 4 of the Metron data set. The blue lines represent all the confirmed tracks for the entire duration of the simulation.

was highly segmented with many missing sections. It should be clear from the results in this paper that there is work to be done to improve results. Further exploration of the other scenarios will hopefully uncover further improvements in the algorithms described in this paper. When the truth for scenario 4 was revealed, there was not any time to further tweak the tracking parameters. The authors are confident that with the knowledge of truth for scenario 4, the tracking metrics can be improved. This will be done in future work.

The authors are investigating other approaches to approximating the maxima of the surface, as well as incorporating other information into the surface. The authors will be exploring the application of Target Strength modeling [3] and Doppler information [12] to the techniques presented in this paper.

Acknowledgment

This work was funded by the U.S. Office of Naval Research, Contract Number N00014-01-G-0460, Delivery Order #36.

References

[1] D. W. Krout, J. W. Pitton, and W. L. J. Fox. Multistatic Sonar Tracking Incorporating Environmentally-

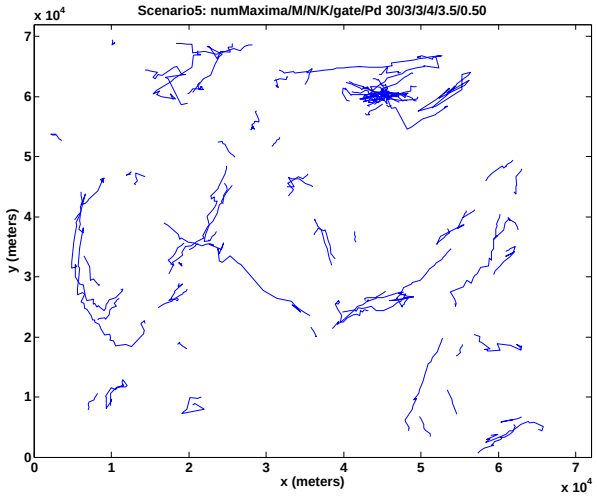

Figure 10: Tracking results for scenario 5 of the Metron data set. The blue lines represent all the confirmed tracks for the entire duration of the simulation.

Adaptive SNR Estimates. In *Proc. Oceans 2006*, Sep. 2006.

[2] J. W. Pitton and W. L. J. Fox. Incorporating Target Strength into Environmentally-Adaptive Sonar Tracking. In *Proc. Oceans 2007*, June 2007.

[3] D. W. Krout and D. Morrison. PDAFAI vs. PDAFAI-wTS: TNO Blind Dataset and SEABAR 07. In *The 12th International Conference on Information Fusion*, July 2009.

[4] F. Ehlers. Final Report on Deployable Multistatic Sonar Systems: NURC-FR-2009-001, NATO UNCLASSIFIED. NATO Undersea Research Center (NURC), January 2009.

[5] F. Ehlers. NURC's Multistatic Sonar Project: NURC-FR-2009-003, NATO UNCLASSIFIED. NATO Undersea Research Center (NURC), February 2009.

[6] D. Lerro and Y. Bar-Shalom. Automated Tracking with Target Amplitude Information. In *Proc. 1990 American Control Conference*, May 1990.

[7] D. Lerro and Y. Bar-Shalom. Interacting Multiple Model Tracking with Target Amplitude Feature. *IEEE Trans. on Aero. and Elect. Systems*, 29(2):494–509, 1993.

[8] K. Orlov. Description of the Metron Simulation data set for the MSTWG. Metron Inc., Released to the MSTWG, June 2009.

[9] Y. Bar-Shalom and M. Scheffe. Sonar Tracking of Multiple Targets using Joint Probabilistic Data Association. *IEEE Journal of Oceanic Engineering*, 8(3):173–184, 1983.

[10] D. L. Hall. *Mathematical Techniques in Multisensor Data Fusion*. Artech House, Norwood, MA, 1992.

[11] S. Coraluppi, D. Grimmett, and P. de Theije. Benchmark Evaluation of Multistatic Trackers. In *The 9th International Conference on Information Fusion*, July 2006.

[12] D. Krout, E. Hanusa, and M. Gupta. Estimation of Position from Multistatic Doppler Measurements. *Submitted to Fusion*, July 2010.